Journal of Magnetic Resonance 213 (2011) 196–199

Contents lists available at SciVerse ScienceDirect

Journal of Magnetic Resonance

journal homepage: www.elsevier.com/locate/jmr

Communication

An efficient amplification pulse sequence for measuring chemical shift anisotropy under fast magic-angle spinning

Ivan Hung, Zhehong Gan *

Center of Interdisciplinary Magnetic Resonance, National High Magnetic Field Laboratory, 1800 East Paul Dirac Drive, Tallahassee, FL 32310, USA

ARTICLE INFO

Article history:
Received 11 July 2011
Revised 25 August 2011
Available online 10 September 2011

Keywords:
Chemical shift anisotropy
CSA
Magic-angle spinning
MAS
Spinning sidebands
Magic-angle turning
MAT
CSA amplification
Extended chemical shift modulation

ABSTRACT

A two-dimensional experiment for measuring chemical shift anisotropy (CSA) under fast magic-angle spinning (MAS) is presented. The chemical shift anisotropy evolution is amplified by a sequence of π-pulses that repetitively interrupt MAS averaging. The amplification generates spinning sideband manifolds in the indirect dimension separated by the isotropic shift along the direct dimension. The basic unit of the pulse sequence is designed based on the magic-angle turning experiment and can be concatenated for larger amplification factors.

1. Introduction

The chemical shift is one of the fundamental spin interactions of NMR spectroscopy. Measuring chemical shift anisotropy (CSA) parameters is of great interest because it can provide not only the magnitude of the spin interaction but also information on the electronic environment surrounding the nucleus [1–3]. For static solids, the orientation dependence of the NMR frequency due to CSA yields the so-called CSA powder pattern from which the three principal tensor components can be measured. For samples with multiple sites, overlap among powder patterns complicates CSA measurement and it is more desirable to perform the measurement under high-resolution magic-angle spinning (MAS) conditions. In the fast spinning regime, CSA powder patterns collapse completely to their isotropic chemical shifts and the anisotropic information is lost. At slow spinning, rotational modulation of the anisotropic chemical shift yields spinning sidebands. The relative intensity of these spinning sidebands can be used to extract CSA parameters, though the appearance of numerous sidebands can cause overlap among different sites, degrading spectral resolution. An ideal solution with the benefits of high spectral resolution and preservation of anisotropic chemical shift information is to separate the CSA and the isotropic shift into two dimensions. Various methods [4–31] have been developed to achieve this goal including recovering CSA using *rf* pulse sequences under fast MAS, rapidly switching the spinning rate or axis, discrete sample hopping, and the methods of phase-adjust sideband separation (PASS) and magic-angle turning (MAT). One class among the methods mentioned above involves applying a sequence of π-pulses that repeatedly interrupt the averaging of CSA by fast MAS. The timing of the pulses can be designed in such a way that the effective evolution results in spinning sidebands which are exactly the same as if the spinning rate is reduced or the CSA is magnified, such sequences have been dubbed extended chemical shift modulation (XCS) [12] or CSA enhancement/amplification in literature [9,32].

In this communication, an efficient CSA amplification sequence that overcomes some of the drawbacks of previous sequences is introduced. The original XCS sequence by Gullion [12] is efficient in terms of the number of pulses required for amplification, but the isotropic chemical shift is also amplified, which can cause problems for samples with multiple sites and/or inhomogeneous broadening. The CSA amplification sequences by Crockford/Shao et al. [33,34] and later by Orr et al. [35] overcame this problem by refocusing the isotropic chemical shift while amplifying the CSA. These sequences were designed following the development path of the PASS experiment, namely, by finding π-pulse timings that satisfy the PASS equations with an amplified CSA and zero isotropic shift evolution. Shao et al. [36] have also shown a modification to the original XCS sequence that compensates the

* Corresponding author. Fax: +1 850 644 1366.
E-mail address: gan@magnet.fsu.edu (Z. Gan).

1090-7807/$ - see front matter © 2011 Elsevier Inc. All rights reserved.
doi:10.1016/j.jmr.2011.09.015

amplified isotropic chemical shift, though the compensation is possible only with a restriction of the t_1 evolution time. A recent review of this topic provides a thorough explanation and comparison of all CSA amplification sequences to date [32]. In this work, a different approach is taken, which does not require solution of any mathematical equations, to the design of CSA amplification sequences that refocus the isotropic chemical shift. The basic unit is based on the magic-angle turning condition, i.e., CSA frequencies at three rotor positions 120° apart average to zero.

For CSA amplification sequences, each π-pulse alternates the sign of time evolution for both the isotropic and anisotropic chemical shifts; this sign alternation interrupts the MAS averaging of CSA. The timing of the π-pulses is designed such that the effective evolution after the accumulated interruption is equivalent to an amplification of the CSA, i.e., the anisotropy $\delta = \delta_{zz} - \delta_{iso}$ ($\delta_{iso} = (\delta_{xx} + \delta_{yy} + \delta_{zz})/3$, $|\delta_{zz} - \delta_{iso}| \geqslant |\delta_{xx} - \delta_{iso}| \geqslant |\delta_{yy} - \delta_{iso}|$) is multiplied by a factor κ, while the asymmetry parameter $\eta = (\delta_{yy} - \delta_{xx})/\delta$ remains unchanged. Fig. 1a shows the basic unit of the original XCS experiment with two π-pulses per rotor period and an evolution time t_1. The π-pulses and corresponding sign alternation of the coherence order double the CSA evolution during t_1, since the CSA evolution would be zero at the end of the rotor period if no sign alternation takes place. Therefore, the unit amplifies the CSA by $\kappa = 2$ and repeating it n times multiplies the CSA evolution by $\kappa = 2n$, achieving efficient CSA amplification. The only drawback of XCS is that the isotropic shift is also amplified by the factor κ because the difference in total duration between the periods of $p = +1$ and -1 coherence order is $\kappa \cdot t_1$ as well. Amplification of the isotropic shift in addition to the CSA results in twisted-phase line shapes and baseline problems for samples with multiple sites and/or inhomogeneous broadening. The removal of isotropic shift evolution during CSA amplification has since been an important focus in the development of newer amplification sequences. This problem has been solved by following the approach used to develop the PASS experiment. By numerically solving the PASS equations for an amplified CSA without isotropic chemical shift evolution, pulse sequences have indeed been found with various numbers of π-pulses, rotor periods and amplification factors [33–36].

The approach taken here to the design of CSA amplification sequences employs the principle behind the magic-angle turning (MAT) experiment, namely, a sum at $N \geqslant 3$ rotor positions $2\pi/N$ apart averages the second-rank CSA. Fig. 1b illustrates the case with $N = 3$, which is the minimum required for second-rank tensors. The π-pulses are divided into two groups. The first group (black) is rotor-synchronous and used to encode CSA evolution. The three encoding pulses amplify CSA evolution by a factor of $\kappa = 6$. The encoding pulses are interspersed with a second group of π-pulses (blue), which satisfy the magic-angle turning condition; hence, these are called MAT pulses. There are several important aspects of the MAT pulses to consider. First, the MAT pulses are introduced to alternate the coherence order between $p = +1$ and -1, such that the CSA evolution from the encoding pulses is cumulative. Second, the MAT condition ensures that the MAT pulses do not themselves contribute to CSA evolution. Third, the MAT pulses can be shifted collectively relative to the rotor-synchronized encoding pulses. This type of shift changes the relative duration between the $p = +1$ and -1 periods and can thus be used to adjust isotropic chemical shift evolution. CSA evolution from the MAT pulses is kept null since the MAT condition remains satisfied. The MAT pulse timings in Fig. 1b are set so isotropic shift evolution is null. Fourth, changes in the order of the MAT pulses have no effect on either the CSA or the isotropic evolution. Fig. 1c shows a modification obtained by shifting the MAT pulses to the right by $\tau_r/6$, such that the first MAT pulse coincides with the first encoding pulse. The two coinciding π-pulses nullify each other, reducing the total number of π-pulses by two. The removal of two π-pulses leaves a blank period, such that a full rotor period can be omitted without affecting the CSA evolution. This modification reduces the basic amplification unit to four π-pulses that occupy two rotor periods, while keeping an amplification factor of $\kappa = 6$. Shifting of the MAT pulses changes the isotropic shift evolution. However, the removal of a complete rotor period makes the total $p = +1$ and -1 periods equal and therefore the isotropic shift is refocused. This is the basic building block employed here for CSA amplification, which can be repeated for larger amplification factors.

Fig. 2 shows the pulse sequence for the 2D CSA amplification experiment. The shortest version consists of two basic units, a stationary and an incrementing unit, separated by an evolution time t_1. The last π-pulse of the first basic unit (i.e., the stationary unit) is removed in order to have a CSA t_1 evolution. This leaves a long blank period such that the incrementing unit can be shifted to

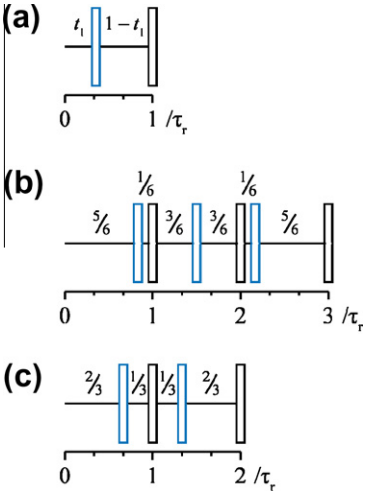

Fig. 1. The basic unit of (a) the original XCS, (b) a CSA amplification sequence with blue pulses satisfying the magic-angle turning condition, and (c) a modification of (b) by shifting the blue pulses to the right by $\tau_r/6$ and taking out the first full rotor period after the shift. The isotropic chemical shift evolution is amplified in (a) and is refocused in (b) and (c). (For interpretation of the references to colour in this figure legend, the reader is referred to the web version of this article.)

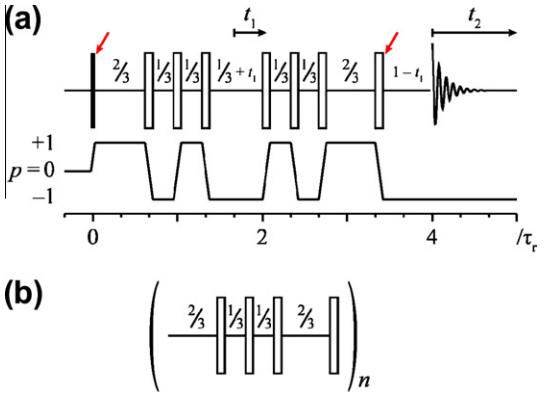

Fig. 2. (a) Pulse sequence and coherence transfer pathway for a $\kappa = 6$ CSA amplification experiment and (b) basic unit for insertion at the positions denoted by red arrows if additional CSA amplification is desired. In (a) a cogwheel phase cycle [37] is employed to select the desired coherence transfer pathway: 0 for all odd-numbered pulses starting from the excitation pulse, $\{0, 1, 2, \ldots 2a + 1\} \times \pi/(a + 1)$ for all even-numbered pulses, and $\{0, \pi\}$ for the receiver phase, where a is the total number of π-pulses. The t_1 increments span exactly one rotor period and a Fourier transformation of t_1 yields spinning sideband intensities corresponding to a spinning rate ν_r/κ. (For interpretation of the references to colour in this figure legend, the reader is referred to the web version of this article.)

the left by one full rotor period resulting in the pulse sequence shown, with seven π-pulses spanning four rotor periods and an amplifications factor of $\kappa = 6$. Cogwheel phase cycling [37] can be applied to select the desired coherence transfer pathway and eliminate artifacts due to imperfect π-pulses. It can be easily verified in the case of $t_1 = 0$ that the $p = +1$ and -1 periods have the same total duration; this condition remains true when incrementing t_1. Therefore, the isotropic chemical shift is always refocused and the indirect dimension only encodes the CSA for this constant-time experiment. Since CSA-only evolution is periodic with the rotor cycle, the t_1 evolution spans one full rotor period to measure spinning sideband intensities. Larger CSA amplification can be achieved by inserting n basic units (shown in Fig. 2b) into both the stationary and incrementing units (positions denoted by red arrows). The resulting amplification factor then becomes $\kappa = 6(n + 1)$.

Fig. 3 demonstrates the 2D ^{13}C CSA amplification experiment using a natural abundance glycine sample. Along the F_2 dimension the 12 kHz MAS yields a spectrum with primarily isotropic peaks. Some intensity remains in the first-order spinning sidebands of the carbonyl site due to its large CSA. Along the F_1 dimension, the CSA amplification yields spinning sideband manifolds for each site. The stacked plot of the 2D spectrum is sheared in such a way that the projection onto the F_2 dimension aligns with a MAS spectrum with a spinning rate of ν_r/κ, as compared in Fig. 3b. It should be noted that the spinning sideband intensities are the same between an amplified CSA ($\kappa \cdot \delta$) or a reduced spinning rate (ν_r/κ). Indeed, the comparison shows a good agreement between the F_2 projection from the CSA amplification experiment and a 1D MAS spectrum acquired at a slow spinning rate equal to ν_r/κ. For the CH_2 site, the peak intensities are attenuated in the 2D amplification spectrum due to the frequency offset effects of the seven π-pulses (the carrier frequency was set on-resonance for the carbonyl peak). If frequency offset due to isotropic shift is a significant fraction of the *rf* field strength, signal attenuation and distortion can become severe due to the compound effect from a large number of π-pulses, especially for the case of large amplification factors. In such cases, it is advisable to only measure the CSA for peaks close to the carrier frequency and perform separate experiments to cover the whole range of isotropic shift. Figs. 3b and c also show the results from larger amplification factors and comparisons with their corresponding slow MAS spectra. These experiments were carried out by inserting additional amplification units (shown in Fig. 2b) at the positions denoted by red arrows in Fig. 2a; for CSA amplification of $\kappa = 12$ and 18, $n = 1$ and 2, respectively. The resulting CSA sideband manifolds from the large amplification factors show good agreement with the slow MAS spectra of corresponding spinning rates ν_r/κ.

It should be noted that the CSA amplification sequence presented here also constitutes a solution of the general PASS equations with amplified CSA and zero isotropic shift evolution. A typical numerical search for solutions of the non-linear PASS equations is not a trivial task, especially for large amplification factors with numerous π-pulses and rotor periods. Orr et al. [35] found a number of solutions but mostly with low amplification factors. For larger amplification factors, they resort to concatenating sequences with low amplification factors. However, this simple approach does not generate the most efficient amplification sequences in terms of the number of π-pulses and/or rotor periods required, as noted in Table 2 of Ref. [35]. Shao et al. [36] have presented a CSA amplification sequence with large κ, which retains the amplification efficiency of XCS (i.e., amplification of $\kappa = 2$ for every pair of π-pulses) while refocusing the isotropic chemical shift. However, this is achieved at the cost of doubling the total number of rotor periods required (compared to XCS) and restricting the number of t_1 increments to $\kappa/2$. This experiment would be most suitable for samples with very small CSA since the highest

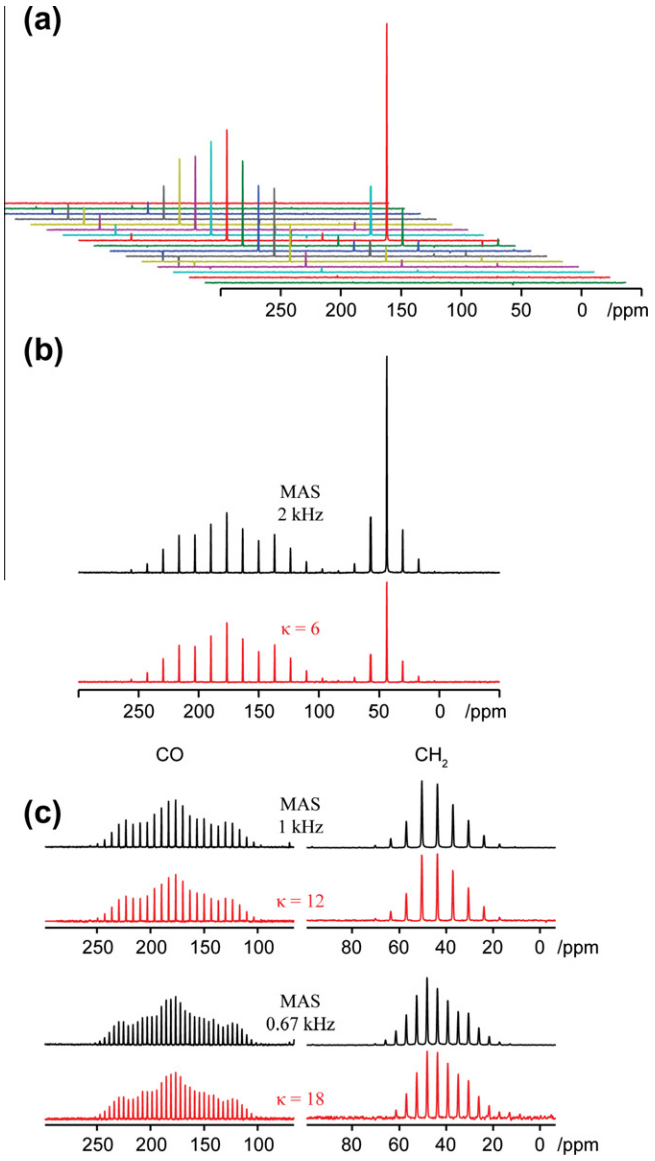

Fig. 3. (a) Stacked-plot of 2D CSA amplification ($\kappa = 6$) spectrum of glycine acquired with $\nu_r = 12$ kHz, (b) comparison of the F_2 projection (red trace) of (a) with a 1D MAS spectrum (black trace) acquired with $\nu_r = 2$ kHz, and (c) Comparison of MAS spectra (black traces, $\nu_r = 1$ kHz (top), $\nu_r = 0.67$ kHz (bottom)) with corresponding F_2 projections of 2D CSA amplification spectra acquired with $\kappa = 12$ and 18 at $\nu_r = 12$ kHz. Experiments were performed on a Bruker Avance 600 spectrometer using a homebuilt 3.2 mm low-E MAS probe [38] with $^1H \rightarrow ^{13}C$ cross-polarization for excitation of the ^{13}C nuclei. The *rf* fields employed for ^{13}C π-pulses and ^1H heteronuclear decoupling are 50 and 100 kHz, respectively. (For interpretation of the references to colour in this figure legend, the reader is referred to the web version of this article.)

number of spinning sidebands that can be obtained is always half of the amplification factor. Implementation of both of the above sequences [35,36] involves pre-calculated delays and is less convenient than the linear t_1 incrementation of conventional 2D experiments.

Crockford/Shao et al. [33,34] take the same approach as in the present work; developing amplification pulse sequences from CSA encoding units that are solutions of the PASS equations. In fact, the basic encoding block shown in Fig. 1c is identical to the solution for $\kappa = 6$ shown by Shao et al. in Table 1 of Ref. [34]. However, the 2D CSA amplification sequences of Crockford/Shao et al. are formed by using a pair of 90° projection-pulses to join the CSA encoding units. The use of projection-pulses causes a factor of

two loss in sensitivity. By joining the CSA encoding units in the way described above, the CSA amplification pulse sequence in Fig. 2a avoids this unnecessary loss, i.e., the sensitivity of the current pulse sequence is improved by a factor of two compared to the analogous experiments presented by Crockford/Shao et al.

In conclusion, a constant-time CSA amplification pulse sequence has been designed based on the magic-angle turning condition. The CSA amplification is efficient in terms of the number of π-pulses and rotor periods required. This 2D experiment can be used to robustly acquire spinning sideband manifolds and measure chemical shift tensors which are completely averaged under high-resolution fast MAS conditions.

Acknowledgments

This work was supported by the National High Magnetic Field Laboratory through National Science Foundation Cooperative Agreement (DMR-0084173) and by the State of Florida.

References

[1] B.J. Wylie, C.M. Rienstra, Multidimensional solid state NMR of anisotropic interactions in peptides and proteins, J. Chem. Phys. 128 (2008) 052207.
[2] H. Saito, I. Ando, A. Ramamoorthy, Chemical shift tensor – the heart of NMR: insights into biological aspects of proteins, Prog. Nucl. Magn. Reson. Spectrosc. 57 (2010) 181–228.
[3] J.C. Facelli, Chemical shift tensors: theory and application to molecular structural problems, Prog. Nucl. Magn. Reson. Spectrosc. 58 (2011) 176–201.
[4] W.T. Dixon, Spinning-sideband-free and spinning-sideband-only NMR-spectra in spinning samples, J. Chem. Phys. 77 (1982) 1800–1809.
[5] A. Bax, N.M. Szeverenyi, G.E. Maciel, Correlation of isotropic shifts and chemical-shift anisotropies by two-dimensional fourier-transform magic-angle hopping NMR-spectroscopy, J. Magn. Reson. 52 (1983) 147–152.
[6] A. Bax, N.M. Szeverenyi, G.E. Maciel, Chemical-Shift anisotropy in powdered solids studied by 2D FT CP MAS NMR, J. Magn. Reson. 51 (1983) 400–408.
[7] T. Terao, T. Fujii, T. Onodera, A. Saika, Switching-angle sample-spinning NMR-Spectroscopy for obtaining powder-pattern-resolved 2d spectra – measurements of C-13 chemical-shift anisotropies in powdered 3,4-Dimethoxybenzaldehyde, Chem. Phys. Lett. 107 (1984) 145–148.
[8] G.E. Maciel, N.M. Szeverenyi, M. Sardashti, Chemical-shift-anisotropy powder patterns by the two-dimensional angle-flipping approach – effects of crystallite packing, J. Magn. Reson. 64 (1985) 365–374.
[9] D.P. Raleigh, A.C. Kolbert, T.G. Oas, M.H. Levitt, R.G. Griffin, Enhancement of the effect of small anisotropies in magic-angle spinning nuclear magnetic-resonance, J. Chem. Soc. Faraday Trans. 1 84 (1988) 3691–3711.
[10] R.C. Zeigler, R.A. Wind, G.E. Maciel, The stop-and-go spinning technique in MAS experiments, J. Magn. Reson. 79 (1988) 299–306.
[11] A.C. Kolbert, D.P. Raleigh, M.H. Levitt, R.G. Griffin, Two-dimensional spin-echo nuclear magnetic-resonance in rotating solids, J. Chem. Phys. 90 (1989) 679–689.
[12] T. Gullion, Extended chemical-shift modulation, J. Magn. Reson. 85 (1989) 614–619.
[13] R. Tycko, G. Dabbagh, P.A. Mirau, Determination of chemical-shift-anisotropy lineshapes in a two-dimensional magic-angle-spinning NMR experiment, J. Magn. Reson. 85 (1989) 265–274.
[14] A.C. Kolbert, R.G. Griffin, 2-dimensional resolution of isotropic and anisotropic chemical-shifts in magic angle spinning NMR, Chem. Phys. Lett. 166 (1990) 87–91.
[15] S.F. Delacroix, J.J. Titman, A. Hagemeyer, H.W. Spiess, Increased resolution in MAS NMR-spectra by 2-dimensional separation of side-band by order, J. Magn. Reson. 97 (1992) 435–443.
[16] L. Frydman, G.C. Chingas, Y.K. Lee, P.J. Grandinetti, M.A. Eastman, G.A. Barrall, A. Pines, Variable-angle correlation spectroscopy in solid-state nuclear-magnetic-resonance, J. Chem. Phys. 97 (1992) 4800–4808.
[17] Z.H. Gan, High-resolution chemical-shift and chemical-shift anisotropy correlation in solids using slow magic angle spinning, J. Am. Chem. Soc. 114 (1992) 8307–8309.
[18] J. Hong, G.S. Harbison, Magic-angle-spinning side-band elimination by temporary interruption of the chemical-shift, J. Magn. Reson. Ser. A 105 (1993) 128–136.
[19] J.Z. Hu, D.W. Alderman, C.H. Ye, R.J. Pugmire, D.M. Grant, An isotropic chemical shift-chemical shift anisotropy magic-angle slow-spinning 2d NMR experiment, J. Magn. Reson. Ser. A 105 (1993) 82–87.
[20] O.N. Antzutkin, S.C. Shekar, M.H. Levitt, 2-dimensional side-band separation in magic-angle-spinning NMR, J. Magn. Reson. Ser. A 115 (1995) 7–19.
[21] J.Z. Hu, W. Wang, F. Liu, M.S. Solum, D.W. Alderman, R.J. Pugmire, D.M. Grant, Magic-angle-turning experiments for measuring chemical-shift-tensor principal values in powdered solids, J. Magn. Reson. Ser. A 113 (1995) 210–222.
[22] Z.H. Gan, R.R. Ernst, An improved 2D magic-angle-turning pulse sequence for the measurement of chemical-shift anisotropy, J. Magn. Reson. Ser. A 123 (1996) 140–143.
[23] D.W. Alderman, G. McGeorge, J.Z. Hu, R.J. Pugmire, D.M. Grant, A sensitive, high resolution magic angle turning experiment for measuring chemical shift tensor principal values, Mol. Phys. 95 (1998) 1113–1126.
[24] Y. Ishii, T. Terao, Manipulation of nuclear spin hamiltonians by rf-field modulations and its applications to observation of powder patterns under magic-angle spinning, J. Chem. Phys. 109 (1998) 1366–1374.
[25] T.M. de Swiet, Three-dimensional measurements of the nuclear magnetic resonance chemical shift and a new analytic data transform for the shift anisotropy, J. Chem. Phys. 112 (2000) 8567–8572.
[26] S.F. Liu, J.D. Mao, K. Schmidt-Rohr, A robust technique for two-dimensional separation of undistorted chemical-shift anisotropy powder patterns in magic-angle-spinning NMR, J. Magn. Reson. 155 (2002) 15–28.
[27] J.C.C. Chan, R. Tycko, Recoupling of chemical shift anisotropies in solid-state NMR under high-speed magic-angle spinning and in uniformly C-13-labeled systems, J. Chem. Phys. 118 (2003) 8378–8389.
[28] .B. Elena, S. Hediger, L. Emsley, Correlation of fast and slow chemical shift spinning sideband patterns under fast magic-angle spinning, J. Magn. Reson. 160 (2003) 40–46.
[29] Y. Nishiyama, A. Kubo, T. Terao, Chemical-shift gamma-encoding nuclear magnetic resonance for uniaxially oriented matter under sample spinning, J. Chem. Phys. 119 (2003) 3297–3308.
[30] M. Strohmeier, D.M. Grant, A new sensitive isotropic-anisotropic separation experiment – SPEED MAS, J. Magn. Reson. 168 (2004) 296–306.
[31] Y. Nishiyama, T. Yamazaki, T. Terao, Development of modulated rf sequences for decoupling and recoupling of nuclear-spin interactions in sample-spinning solid-state NMR: application to chemical-shift anisotropy determination, J. Chem. Phys. 124 (2006) 64304.
[32] L. Shao, J.J. Titman, Chemical shift anisotropy amplification, Prog. Nucl. Magn. Reson. Spectrosc. 51 (2007) 103–137.
[33] C. Crockford, H. Geen, J.J. Titman, Two-dimensional MAS-NMR spectra which correlate fast and slow magic angle spinning sideband patterns, Chem. Phys. Lett. 344 (2001) 367–373.
[34] L.M. Shao, C. Crockford, H. Geen, G. Grasso, J.J. Titman, Chemical shift anisotropy amplification, J. Magn. Reson. 167 (2004) 75–86.
[35] R.M. Orr, M.J. Duer, S.E. Ashbrook, Correlating fast and slow chemical shift spinning sideband patterns in solid-state NMR, J. Magn. Reson. 174 (2005) 301–309.
[36] L.M. Shao, C. Crockford, J.J. Titman, Chemical shift anisotropy amplification with high amplification factor and improved sensitivity, J. Magn. Reson. 178 (2006) 155–161.
[37] M.H. Levitt, P.K. Madhu, C.E. Hughes, Cogwheel phase cycling, J. Magn. Reson. 155 (2002) 300–306.
[38] S.A. McNeill, P.L. Gor'kov, K. Shetty, W.W. Brey, J.R. Long, A low-E magic angle spinning probe for biological solid state NMR at 750 MHz, J. Magn. Reson. 197 (2009) 135–144.